THE MEASUREMENT OF FIBRIL ANGLE OF WOOD FIBERS USING POLARIZED LIGHT

F. El-Hosseiny and *D. H. Page*
Pulp and Paper Research Institute of Canada, Pointe Claire, Quebec

(Received 10 August, 1973)

ABSTRACT

The fibril angle of the S_2 layer of wood pulp fibres can be determined microscopically from the extinction position of intact cell walls between crossed polars. It is always assumed in this method that the S_1 and S_3 layers are so thin that they do not affect the state of polarization of light.

The complete theory of the extinction position has been derived, taking into account the contribution of the S_1 and S_3 layers, for the light path used in the mercury reflectance method of Page. For certain thicknesses of the S_2 layer, the presence of the S_1 and S_3 layers can introduce serious errors in the fibril angle measurement. However, there is a range of S_1, S_2, and S_3 thicknesses for which the error is small and the fibres of most softwoods lie within this range. For thick-walled species the method must be used with caution.

Additional keywords: cell-wall models, wall layers, softwoods, birefringence, mercury

INTRODUCTION

The structure of a wood fibre is shown in Fig. 1 (Kerr and Bailey 1934). Apart from a tenuous primary wall P, it consists of three secondary layers S_1, S_2, and S_3 of varying thickness. Each layer is composed of long substantially crystalline cellulosic fibrils embedded in an amorphous matrix of hemicellulose and lignin. The fibrils of the S_1 and S_3 layers are approximately perpendicular to the fibre axis, whereas those of the S_2 layer wrap around the fibre axis in a steep helix. The angle of the helix, termed the fibril angle, varies between fibres, but is approximately constant within a fibre.

The S_2 layer is by far the thickest of the layers so that its fibril angle is important in the study of the physical behaviour of fibres and wood. For example, the stress-strain relations of a fibre depend on its fibril angle (Page et al. 1972); the shrinkage behaviour of a piece of wood depends on the mean fibril angle of its fibres (Harris and Meylan 1965). Several methods have been developed for the measurement of fibril angle, including X-ray diffraction, electron microscopy, and various techniques of light microscopy. These methods are listed in Page (1969).

Some of the light microscopical techniques make use of the natural birefringence of cellulose. The fibril direction in a portion of the cell wall can be readily obtained by examination between crossed polars. Upon rotation of the specimen, the transmitted intensity falls to zero when the fibrils are parallel to one of the polars. This procedure cannot be used for intact fibres because the opposite sides of a helically wound cell wall interfere. This objection has been overcome in a number of ways, for example by observation of extinction of a single wall through a bordered pit, and by observation of a single wall obtained by longitudinal sectioning. A more general, rapid, nondestructive technique was developed by Page (1969). In this method observation of a single wall is made by reflecting light from drops of mercury introduced into the lumen. The light path is shown diagrammatically in Fig. 2.

The polarized light methods all assume that extinction occurs when the fibrils in the S_2 layer are parallel to the polarizer (or analyzer). This is only strictly true, however, if the thicknesses of both the S_1 and S_3 layers are zero. It has been assumed in previous work that the S_1 and S_3 layers are sufficiently thin to have a negligible effect

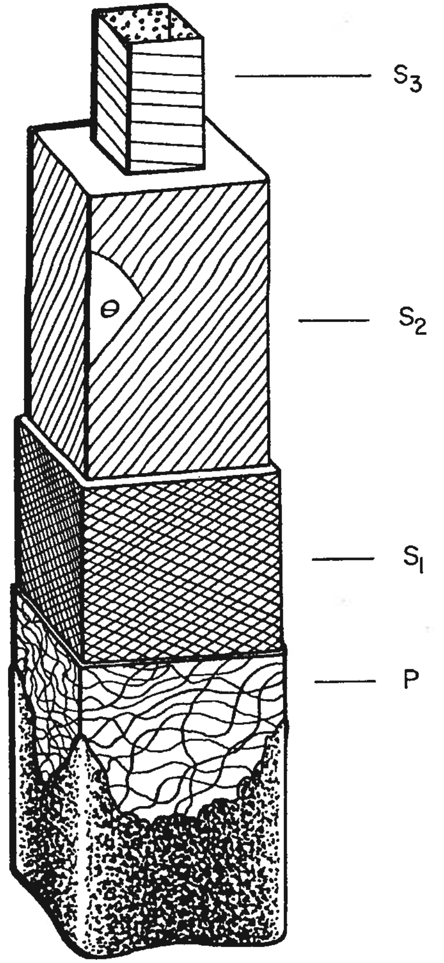

FIG. 1. Schematic representation of a single fibre of wood showing the arrangement of the cellulosic microfibrils in the various layers of the cell wall.

on the determination of the fibril angle. Recent work by the authors has indicated that in certain circumstances this may be an unjustifiable assumption. It is the purpose of this paper to examine theoretically the effect of S_1 and S_3 thickness on the extinction behaviour of a single cell wall when viewed in reflected light.

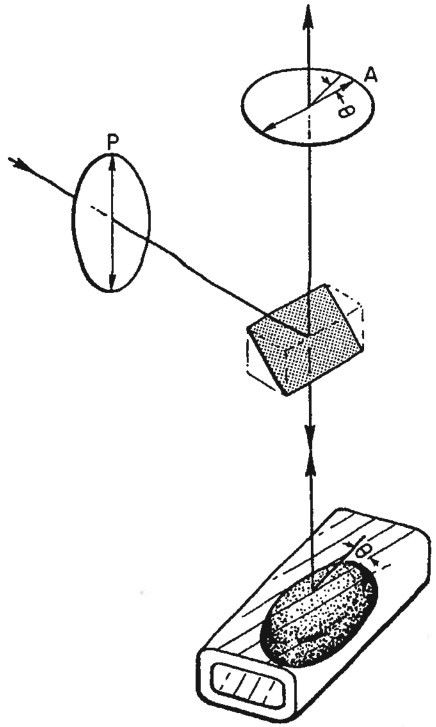

FIG. 2. Light path for method of Page (1969). Light is reflected from the mercury drop in the lumen. Extinction occurs with crossed polars when the fibril direction in the S_2 layer is parallel to the polarizer or analyzer, provided that the existence of the S_1 and S_3 layers is ignored.

THEORY

The detailed path of light through the cell wall is shown in Fig. 3. The incident ray passes through the S_1, S_2, and S_3 layers, is reflected at the mercury surface, and is returned through the S_3, S_2, and S_1 layers. The theory of the intensity of light emerging from such a system will now be presented.

The geometrical relationships between the analyzer and polarizer directions, the fibre axis, and the direction of the fibrils in each layer are represented in Fig. 4. The fibrils of S_2 make an angle θ with the fibre axis. The S_1 layer is generally considered

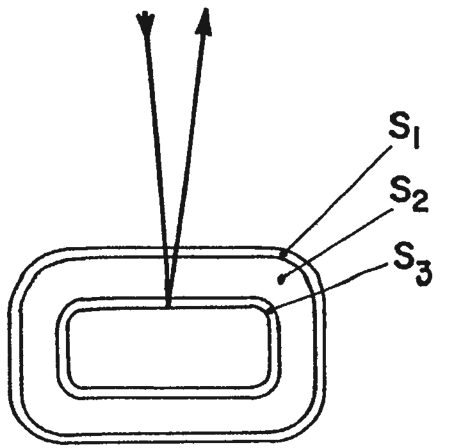

Fig. 3. Actual light path for method of Page. Light traverses the layers in the sequence S_1, S_2, S_3, S_3, S_2, S_1.

to comprise several layers of fibril angle 70–80° with alternating S and Z helices. The optical behaviour of such a structure is approximately equivalent to a single layer of fibril angle 90°. For the analysis given here, the fibrils of S_1 are thus assumed to be perpendicular to the fibre axis. The S_3 layer is treated similarly. We wish to consider the variation of intensity of reflected light as the fibre is rotated. For convenience we chose as a parameter of rotation

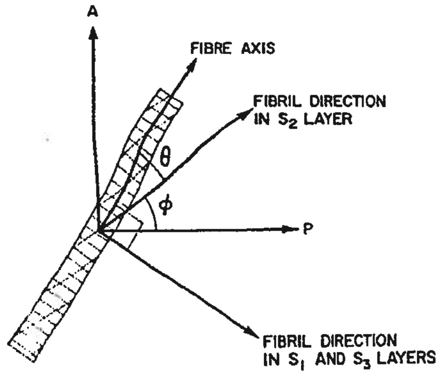

Fig. 4. Relation of fibril direction in the S_1, S_2, and S_3 layers to the directions of the polarizer and analyzer.

the angle ϕ, the angle between the S_2 fibril direction and the polarizer P.

Hsü et al. (1947) derived the intensity of light emerging from n birefringent plates between a polarizer and analyzer. Applying this to our problem, we obtain the following equation:

$$\begin{aligned} I = I_0[&\sin 2\phi \sin 2\gamma_2 \cos \gamma_1 \cos (\gamma_1 + 2\gamma_3) \\ &- \sin 2(\phi + \theta)\{\sin 2\gamma_1 \cos 2\gamma_2 \cos 2\gamma_3 \\ &\qquad + \cos 2\gamma_1 \cos^2 \gamma_2 \sin 2\gamma_3\} \\ &- \sin 2(\phi + 2\theta) \sin(\gamma_1 + 2\gamma_3) \sin \gamma_1 \sin 2\gamma_2 \\ &- \sin^2 \gamma_1 \sin^2 \gamma_2 \sin 2\gamma_3 \sin 2(\phi + 3\theta) \\ &+ \cos^2 \gamma_1 \sin^2 \gamma_2 \sin 2\gamma_3 \sin 2(\phi - \theta)]^2 \end{aligned} \quad (1)$$

where $\gamma_1 = (\pi/\lambda)\mu t_1$; $\gamma_2 = (\pi/\lambda)\mu t_2$; $\gamma_3 = (\pi/\lambda)\mu t_3$

μ is the birefringence of the cell wall (assumed to be the same for all layers);

λ is the wavelength of the incident monochromatic light;

t_1, t_2, and t_3 are the thicknesses of the S_1, S_2, and S_3 layers, respectively;

I is the transmitted light intensity and I_0 is the intensity of light incident on the specimen.

The position of the fibre at minimum transmitted intensity is obtained by equating $dI/d\phi$ to zero. Then $\phi = \epsilon$ where

$$\tan 2\epsilon = \frac{A}{B} \quad (2)$$

and

$$\begin{aligned} A = &\sin 6\theta \sin^2 \gamma_1 \sin^2 \gamma_2 \sin 2\gamma_3 \\ &+ \sin 4\theta \sin (\gamma_1 + 2\gamma_3) \sin \gamma_1 \sin 2\gamma_2 \\ &+ \sin 2\theta(\sin 2\gamma_1 \cos 2\gamma_2 \cos 2\gamma_3 \\ &\qquad + \cos 2\gamma_1 \cos^2 \gamma_2 \sin 2\gamma_3 \\ &\qquad + \cos^2 \gamma_1 \sin^2 \gamma_2 \sin 2\gamma_3) \end{aligned} \quad (2a)$$

$$\begin{aligned} B = &\sin 2\gamma_2 \cos \gamma_1 \cos (\gamma_1 + 2\gamma_3) \\ &- \cos 6\theta \sin^2 \gamma_1 \sin^2 \gamma_2 \sin 2\gamma_3 \\ &- \cos 4\theta \sin (\gamma_1 + 2\gamma_3) \sin \gamma_1 \sin 2\gamma_2 \\ &- \cos 2\theta(\sin 2\gamma_1 \cos 2\gamma_2 \cos 2\gamma_3 \\ &\qquad + \cos 2\gamma_1 \cos^2 \gamma_2 \sin 2\gamma_3 \\ &\qquad - \cos^2 \gamma_1 \sin^2 \gamma_2 \sin 2\gamma_3) \end{aligned} \quad (2b)$$

Because Eq. (1) is a complete square of the function ϕ, then the minimum intensity given by Eq. (2) must be zero for all values of γ, θ, and S_1, S_2 and S_3 thicknesses. Thus the composite sandwich behaves as a single crystal. However, the extinction direction of the sandwich differs from the direction of the S_2 fibrils by the angle ϵ, which can thus be regarded as the error involved in using the extinction direction of the composite as a measure of the fibril angle of the S_2 layer. We shall use the term "apparent fibril angle" to denote the angle between the extinction direction and the fibre axis—the "fibril angle" as measured by the method described by Page.

Application of the theory to specific cases

The magnitude of error in fibril angle is given by Eq. (2). Unfortunately, this equation is a complex function of fibril angle, wavelength, and wall thicknesses, so that it is not possible to present an overall picture of the variation in error. The error has therefore been computed for certain specific cases.

Effect of cell-wall thickness

The thickness of the S_2 layer is treated as the principal variable, and its effect on error is computed for five different combinations of S_1 and S_3 thickness. In each instance we consider monochromatic light of wavelength 540 nm. The birefringence of the cell-wall material of wood has been measured and found to be about 0.045. This rises to 0.060 upon delignification. For these calculations we have adopted the latter value.

1. *Fibres with no S_3 layer, and with an S_1 layer of constant thickness of 0.2 μm.* Figure 5(a) shows the apparent fibril angle as a function of S_2 layer thickness for an actual fibril angle of 10°. The fibril angle is measured correctly only when the thickness of the S_2 layer is 2.25 μm. For thinner S_2 layers the angle is overestimated and for thicker layers it is underestimated. A discontinuity occurs when the S_2 thickness is 4.50 μm. At this thickness the retardation of light in passing twice through the S_2 layer is exactly one wavelength, and the apparent fibril angle is 90°, that of the S_1 layer. With increasing S_2 thickness, the same graph is repeated. The error in fibril angle is no greater than 1° for fibres of S_2 thickness lying between 1.3 and 3.4 μm.
   Figure 5(b) shows a similar plot for an actual fibril angle of 30°. The error in fibril angle is no greater than 3° for fibres of S_2 thickness lying between 1.3 and 3.4 μm. However, again, very considerable errors can occur for fibres outside these limits.
2. *Fibres with no S_3 layer, and with S_1 layers that are 10% of the thickness of the S_2 layer.*
   Figure 6 shows the apparent fibril angle as a function of S_2 thickness for an actual fibril angle of 30°. The pattern is similar to Case 1, except that the

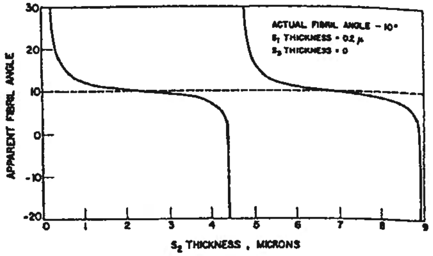

Fig. 5a. Effect of cell-wall thickness on apparent fibril angle—case 1.

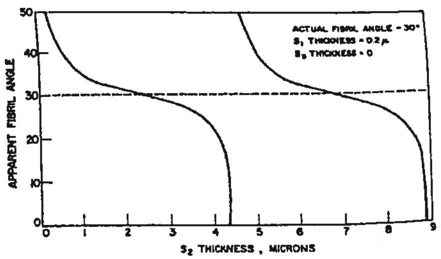

Fig. 5b. Effect of cell-wall thickness on apparent fibril angle—case 1.

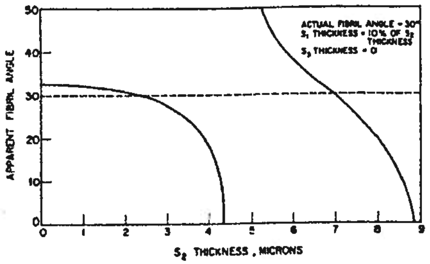

FIG. 6. Effect of cell-wall thickness on apparent fibril angle—case 2.

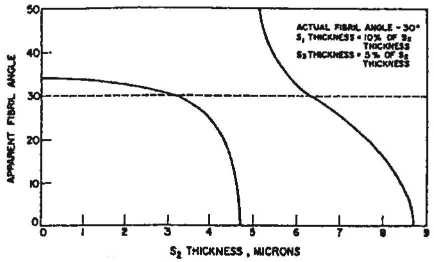

FIG. 8. Effect of cell-wall thickness on apparent fibril angle—case 4.

error remains small for thin S_2 layers. The error is no greater than 3° for thicknesses between 0 and 3.4 μm.

3. *Fibres with an S_3 layer that is equal in thickness to the S_1 layer. Both layers are 5% of the thickness of the S_2 layer.* Figure 7 shows the apparent fibril angle as a function of S_2 thickness for an actual fibril angle of 30°. In this case, the discontinuity at 4.5 μm disappears and the error does not exceed 3° over the wide range of thicknesses from 0–6.3 μm.

4. *Fibres with an S_3 layer that is thinner than the S_1 layer. S_1 is 10% and S_3 5% of the thickness of the S_2 layer.* Figure 8 shows the apparent fibril angle as a function of S_2 thickness for an actual fibril angle of 30°. The behaviour is similar to Case 2, where there is no S_3 layer. The error in fibril angle is less than 3° for S_2 thicknesses between 1.3 and 3.8 μm.

5. *Fibres with an S_3 layer that is thicker than the S_1 layer. S_3 is 10% and S_1 5% of the thickness of the S_2 layer.* Figure 9 shows the apparent fibril angle as a function of S_2 thickness for an actual fibril angle of 30°. Under these conditions there is no S_2 thickness for which the fibril angle is correctly measured. The error is less than 5° for thicknesses between 0 and 3.4 μm.

Effect of wavelength

Here we shall consider a fibre with no S_3 layer and with the S_1 layer 20% of the S_2 layer. Four thicknesses of the S_2 layer are considered, 2.27 μm, 4.55 μm, 6.83 μm, and 9.10 μm.

Figure 10 shows theoretical curves of the effect of wavelength on apparent fibril angle, for an actual fibril angle of 30°. For the thinnest S_2 layer, the error in fibril angle is small and is independent of wavelength over the range normally used. For thicker

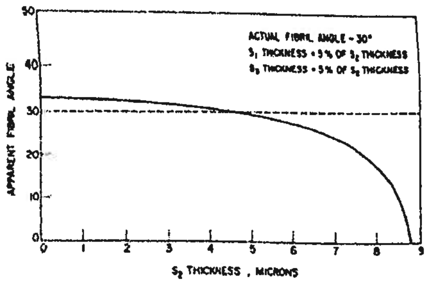

FIG. 7. Effect of cell-wall thickness on apparent fibril angle—case 3.

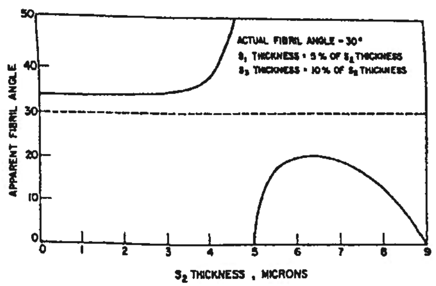

FIG. 9. Effect of cell-wall thickness on apparent fibril angle—case 5.

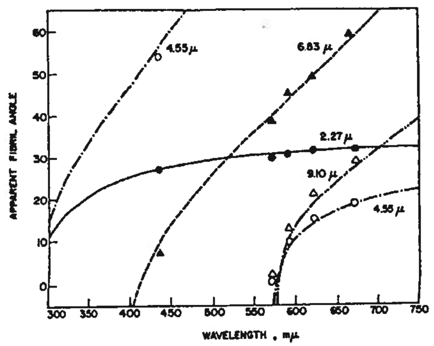

FIG. 10. Effect of wavelength on apparent fibril angle for four thicknesses of the S_2 layer (2.27 μm, 4.45 μm, 6.83 μm and 9.10 μm). The S_1 layer is assumed to be 20% of the S_2 layer. The lines are theoretical, and the points determined experimentally using a model system.

fibres the error is generally large and is a strong function of wavelength. The apparent fibril angle is greater for higher wavelengths. Thus for thick-walled fibres, dispersion of the extinction position would occur in white light. As the fibre is rotated, a spectrum of colours would be seen and at no point would a complete extinction occur for all wavelengths.

Experimental verification

The theoretical calculations were checked in a single experiment using a model system. The S_1 and S_2 layers of a fibre were simulated by a cellulose acetate sheet and a quartz plate of known thickness and birefringence respectively, set with their optical axes at 60° to each other to simulate a fibre of fibril angle 30°. The plates were examined under polarized vertical illumination in a microscope, using a mirror beneath the plates to reflect the light. The extinction position, and hence the apparent "fibril angle," was determined over a range of wavelengths from 436–670 nm.

The results are shown as points in Fig. 10 superimposed on the theoretically determined curves. The data points fit the theoretical lines excellently.

Qualitative verification is obtained from direct observation of single fibres. Thick-walled fibres exhibit dispersion of the extinction position as predicted in Fig. 10. There is no extinction position in white light, but a spectrum of colours is seen as the fibre is rotated. The phenomenon is common for the very thick-walled summerwood fibres of the southern pines, but fibres of the thin-walled northern softwoods generally show good extinction in white light.

DISCUSSION

The assumption that the extinction angle is equal to the S_2 fibril angle in the mercury reflectance method of Page is not generally valid. The birefringent S_1 and S_3 layers although thin cannot be ignored. When they are taken into account, it is found that an extinction position always occurs in monochromatic light, but the S_2 fibrils are not then exactly parallel to the polarizer or analyzer. The theory indicates that for certain conditions the error in determination of fibril angle can be very large.

It is important to recognize these limitations in terms of the actual conditions that apply for wood pulp fibres. The error is small if the S_1 and S_3 layers are thin and if the S_2 layer thickness lies between 1.3 and 3.4 μm. Fortunately, these are conditions that apply to the great majority of softwood fibres. Generally the S_1 layer is thin. Its thickness has been reported as 0.14 μm (Emerton and Goldsmith 1956), 0.20 μm (Meier 1955) and between 0.12 and 0.35 μm (Jayme and Fengel 1962). We have concluded that a mean thickness of 0.20 μm is general for most softwood species. The S_3 layer is generally thinner than the S_1 layer and in some species is almost nonexistent. Values of 0.07–0.08 μm (Jayme and Fengel 1962) and 0.10–0.15 μm (Liese 1960) have been obtained for various softwoods.

For species of spruce, red cedar, balsam fir, white pine, and Douglas-fir over 95% of the fibres have S_2 thicknesses between 1.0 and 3.5 μm. Moreover, the mean S_2 thickness is about 2.0–2.5 μm, which is the region in which the error is less than 1°.

For some very thick-walled species, these conditions do not apply. The summerwood fibres of southern pines, for example, often have S_2 thicknesses in the range 3.5–5.5 μm, and the S_1 and S_3 layers are also thick, so that the method fails for these fibres.

CONCLUSIONS

The use of the extinction position of the intact cell wall for the determination of fibril angle, as developed in the method of Page, must be used with care. An error arises because of the birefringent S_1 and S_3 layers. The error in the determination is small for fibres with thin S_1 and S_3 layers ($<$0.20 μm) and S_2 layers in the range 1.3–3.4 μm. These conditions apply to most fibres of most softwoods, but certain species, such as the southern pines, have many fibres that exceed the upper limit of S_2 layer thickness. Such fibres show dispersion of the extinction position in white light, and this serves as a warning that the technique should not be used.

REFERENCES

EMERTON, H. W., AND V. GOLDSMITH. 1956. The structure of the outer secondary wall of pine tracheids from kraft pulps. Holzforschung 10:108.

HARRIS, J. M., AND B. A. MEYLAN. 1965. The influence of microfibril angle on longitudinal and tangential shrinkage in *Pinus radiata*. Holzforschung 19:144–153.

HSÜ, HSIEN-YÜ., M. RICHARTZ, AND YÜNG-K'ANG LIANG. 1947. A generalized intensity formula for a system of retardation plates. J. Opt. Soc. Am. 37:99.

JAYME, G., AND D. FENGEL. 1962. Elektronenoptische Beobachtungen über den Feinbau von Nadelholzzellen. Pap Darmst. 16 (10a):519.

KERR, T., AND I. W. BAILEY. 1934. The cambium and its derivative tissues. No. X. Structure, optical properties and chemical composition of the so-called middle lamella. J. Arnold Arboretum 15:327.

LIESE, W. 1960. The structure of the tertiary wall in tracheids and wood fibres. Holz. Roh-Werkst. 18:296.

MEIER, H. 1955. Uber den Zellwandabbau durch Holzvermorschungspilze und die submikroskopische struktur von Fichtentracheiden und Birkenholzfasern. Holz. Roh- Werkst. 13:323.

PAGE, D. H. 1969. A method for determining the fibrillar angle in wood tracheids. J. Roy Microscop. Soc. 90(2):137–143.

PAGE, D. H., F. EL-HOSSEINY, K. WINKLER AND R. BAIN. 1972. The mechanical properties of single wood-pulp fibres. Part I: A new approach. Pulp Pap. Mag. Can. 73 (8):T198–T203.

THREE-DIMENSIONAL FINITE-ELEMENT MODELS OF CYLINDRICAL WOOD FIBERS

J. D. Barrett

Department of the Environment, Canadian Forestry Service
Western Forest Products Laboratory, Vancouver, British Columbia

and

A. P. Schniewind

University of California, Forest Products Laboratory, Richmond, California

(Received 5 July 1973)

ABSTRACT

A finite-element solution is presented for analysis of concentric, multilayered, orthotropic cylinders subjected to loadings that do not vary around the circumference. Model fibers are analyzed, and stress distributions are compared to those obtained, using a closed form solution technique. The influence of boundary-shear restraint on internal stress distribution is studied. Comparing results of the three-dimensional finite-element model to values of axial stiffness and relative twisting angles predicted using simpler, two-dimensional methods indicated that the two-dimensional models can give good estimates of these parameters, at least for the thin-walled models.

Additional keywords: Mathematical analysis, layered systems, finite element, cell mechanics.

Symbols

A	Cell-wall cross-section area
B	Strain matrix
C_{ij}	Elastic compliances
D	Matrix of elastic compliances
E_{rr}, E_{tt}, E_{zz}	Moduli of elasticity
G_{rt}, G_{rz}, G_{tz}	Shear moduli of elasticity
P	External axial force
P_j	Layer volume proportion
p	Internal or external pressure
r,t,z	Coordinate directions
$\hat{S}_{ij}$	Composite-layer compliance component
u,v,w	Displacement components
u_i, v_i	Nodal displacements
$v_{2.0}$	Displacement at $z = 2.0$ cm
α	An angle
$\gamma_{rt}, \gamma_{rz}, \gamma_{tz}$	Shear strain components
δ	Vector of element displacement components
$\epsilon_{rr}, \epsilon_{tt}, \epsilon_{zz}$	Normal strain components
ϵ_0	Specified strain component
η, ξ	Local element coordinates
θ	Coordinate direction
μ_{ij}	Poisson's ratios
$\sigma_{rr}, \sigma_{tt}, \sigma_{zz}$	Normal stress components
$\sigma_{rt}, \sigma_{rz}, \sigma_{tz}$	Shear stress components
$\bar{\sigma}$	Axial stress
ϕ	Twist angle

Superscripts

′(prime)	Coordinate system parallel and perpendicular to microfibrils
e	Element property
T	Transpose of vector or matrix quantity

Subscript

j	j[th] layer property

INTRODUCTION

In approaching the three-dimensional elastic analysis of wood fibers, the simplest logical geometric model appears to be the circular cylinder. Solutions for the distribution of stresses and displacements in circular isotropic and orthotropic cylinders have been available for many years for some specific loading conditions (Timoshenko and Goodier 1951; Lekhnitskii 1963). A general treatment of the state of stresses in a multilayered system of concentric, anisotropic cylinders subjected to axial